Progress in Neuropsychopharmacology & Biological Psychiatry 89 (2019) 254–262

Contents lists available at ScienceDirect

Progress in Neuropsychopharmacology & Biological Psychiatry

journal homepage: www.elsevier.com/locate/pnp

Insular changes induced by electroconvulsive therapy response to symptom improvements in schizophrenia

Yuchao Jiang[a,1], Mengqing Xia[b,1], Xiangkui Li[a], Yingying Tang[b], Chunbo Li[b,c], Huan Huang[b], Debo Dong[a], Sisi Jiang[a], Jijun Wang[b,c,*], Jian Xu[d,*], Cheng Luo[a,**], Dezhong Yao[a]

[a] The Clinical Hospital of Chengdu Brain Science Institute, MOE Key Lab for Neuroinformation, Center for Information in Medicine, School of life Science and technology, University of Electronic Science and Technology of China, Chengdu 610054, China
[b] Shanghai Key Laboratory of Psychotic Disorders, Shanghai Mental Health Center, Shanghai Jiaotong University School of Medicine, Shanghai 200030, China
[c] Bio-X Institutes, Key Laboratory for the Genetics of Developmental and Neuropsychiatric Disorders (Ministry of Education), Shanghai Jiaotong University, Shanghai 200030, China
[d] Department of Neurology, Nantong University Affiliated Mental Health Center, Jiangsu, Nantong 226005, People's Republic of China

ARTICLE INFO

Keywords:
Electroconvulsive therapy
Schizophrenia
Insula
MRI
Resting-state functional connectivity

ABSTRACT

Although modified electroconvulsive therapy (MECT) has been employed as a treatment strategy and to resolve medication resistant symptoms in schizophrenia (SZ), its action mechanisms remain unclear. The insula has been demonstrated to associate with clinical symptoms and neuropathology in SZ. This study examined whether insular changes response to MECT outcomes in SZ. Forty-two SZ were divided into two groups according to their treatment strategies. One group (MSZ, n = 21) received 4-weeks MECT together with antipsychotics; another group (DSZ, n = 21) was treated only with antipsychotics. Twenty-three healthy controls (HC) were also included. Structural and functional MRI were scanned twice (baseline and after 4-week treatment) for SZ and once for HC. Firstly, the insula was divided into three subregions based on resting-state functional connectivity (FC). Subsequently, gray matter volume (GMV) and voxel-wise FC were assessed in each subregion. Finally, the relationship between insular changes and symptom improvements was also investigated. Compared with baseline, the DSZ group showed reduced GMV in insular subregions. In contrast, the MSZ group exhibited increased GMV in bilateral posterior insula (PIns); furthermore, the increase in the PIns was correlated with symptom improvements. Second, the decreased FC between right PIns and left orbitofrontal cortex, and left PIns and middle occipital gyrus was observed only in the MSZ group; moreover, these FC changes were associated with symptom improvements. The present study demonstrated that MECT induced insular changes, which may contribute to the mechanisms of MECT.

1. Introduction

Modified electroconvulsive therapy (MECT) is one of the most effective treatments in mood disorders (Fochtmann, 2016). To data, MECT is also employed as an augmentation of antipsychotic treatment and to resolve medication resistant symptoms in schizophrenia (SZ) (Petrides et al., 2015). Although it has been seven decades after the introduction of MECT in the field of psychiatry, its mechanisms of action on brain remain unclear. Recently, neuroimaging studies have provided accumulated evidence regarding the modulation of MECT on brain structure, such as the medial temporal lobe (Abbott et al., 2014; Takamiya et al., 2018) and prefrontal cortical regions (Bouckaert et al., 2016; Thomann et al., 2017) in depressive disorder. One potential underlying mechanism is the neuroplasticity in these pivotal regions (Bouckaert et al., 2014), which are affected in the psychiatric disorders. Some type of physiologic tissue reaction to the electric current is considered as another potential reason for the efficacy of MECT such as edema of neurons in the target regions (Andrade and Bolwig, 2014). Previous studies have shown that a combination of MECT and antipsychotics has a remarkable advantage in terms of the rapidity and quality of response in SZ (Abraham and Kulhara, 1987); however, few studies have focused on the MECT-effects on brain structure and

* Corresponding authors.
** Corresponding author at: The Clinical Hospital of Chengdu Brain Science Institute, MOE Key Lab for Neuroinformation, Center for Information in Medicine, School of life Science and technology, University of Electronic Science and Technology of China, Chengdu 610054, China.
E-mail addresses: jijunwang27@163.com (J. Wang), xujianr@163.com (J. Xu), chengluo@uestc.edu.cn (C. Luo).
[1] Yuchao Jiang and Mengqing Xia contributed equally to this study.

https://doi.org/10.1016/j.pnpbp.2018.09.009
Received 27 June 2018; Received in revised form 10 September 2018; Accepted 19 September 2018
Available online 21 September 2018

resting-state functional connectivity (FC) in SZ. In addition, the relationship between these brain changes induced by MECT and clinical symptoms improvement has not been reported in schizophrenia.

To date, broad cortical abnormalities have been identified in SZ; however, a wide range of knowledge has centered on insular disturbances (Jiang et al., 2017; Moran et al., 2013; Palaniyappan et al., 2013). A substantial number of studies have suggested that functional and structural alterations of the insula play a critical role in leading to the clinical features of SZ (Menon, 2011; Uddin, 2015). The insula was considered a key node of the salience network (salience monitoring), which was included in a systematic triple network model to synthesize extant findings for understanding dysfunction in the insula across multiple psychiatric disorders (Menon, 2011). The compelling evidence originated from several studies that illustrated a reduction in the strength of the causal influences from the salience network to the frontoparietal network (goal-oriented or externally directed cognition) and default network (self-related or internally directed cognition) in SZ (Palaniyappan et al., 2013). Furthermore, based on the findings of our recent meta-analysis of seed-based resting state functional connectivity, we proposed a disconnected large-scale brain network model of SZ in which the salience processing network plays the core role, and its imbalanced communication with other functional networks may underlie the dissociation between self-representation and environmental salience processing (Dong et al., 2017). In addition, altered gray matter features of the insula have been observed in SZ (Honea et al., 2005; Jiang et al., 2018a). A recent review emphasized that deficits in the insula may be highly relevant to the symptoms and pathobiology of SZ (Wylie and Tregellas, 2010). Furthermore, insular neuroplasticity has been identified in structural and functional imaging investigations (He et al., 2018a, 2018b; Luo et al., 2014). Thus, increasing attention has been paid to the pathological roles of the insula in SZ; however, the potential effects of MECT on the structural and functional changes in the insula in SZ has not been previously investigated. According to insular connectivity, function and cytoarchitecture, the whole insular cortex may be divided into three subregions: the dorsal anterior insula (dAIns), the ventral anterior insula (vAIns) and the posterior insula (PIns) (Chang et al., 2013). Previous schizophrenia research have indicated that SZ showed specific alterations for insular subregions. For example, Chen and colleagues found that the PIns of SZ had altered functional connections with the thalamus and primary sensorimotor area (Chen et al., 2016). Moran and colleagues indicated the disruption of right dAIns modulation of central executive and default mode networks in SZ (Moran et al., 2013). Therefore, it is considerable to investigate the effect of ECT on different insular subregions.

To systematically determine the effect of MECT on the changes in the structure and function of the insula in SZ, a longitudinal study was designed according to the previous study (Redlich et al., 2016) which is presented in the Fig. 1. The structural and resting-state functional magnetic resonance imaging (MRI) data were collected at pre-treatment and post-treatment. We initially employed a clustering method from our previous study (Cao et al., 2014; Chen et al., 2016) to divide the insula into three subregions based on resting-state FC profiles. Gray matter volume (GMV) and voxel-wise FC in each insular subregions were used to assess the structural and functional changes in patients before and after treatment with MECT. We also investigated whether these brain changes induced by MECT correlated with clinical improvements.

2. Experimental procedures

2.1. Participants

Two groups of inpatients with acute schizophrenia were recruited in parallel in Shanghai Mental Health Center (SMHC). Only the patients who were identified as medication-resistant according to their previous treatment history were administered a 4-week ECT in combination with antipsychotics (being assigned to ECT group, MSZ group, n = 21). Informed consent on ECT was obtained from each patient and his/her family. The patients who were not medication-resistant or did not agree to receive ECT were managed with only antipsychotics (being assigned to drug group, DSZ group, n = 21). Both groups were matched by sex, age, education levels, and baseline psychiatric symptoms. Patients with very severe psychiatric symptoms such as significant psychomotor excitement had been excluded because of tolerance to long duration of MRI scan. All the patients were recruited from October 2013 to January 2015. The patients were diagnosed with SZ by trained clinical psychiatrists using the SCID-I/P (Structural Clinical Interview for DSM-IV-TR, Patient's version). In addition, the patients had no history of MECT within the previous six months. Psychiatric symptom severity was assessed by The Positive and Negative Syndrome Scale (PANSS), and the total PANSS scores of all patients were > 60. All patients received antipsychotic medications, and the daily antipsychotic medication dosage was converted to chlorpromazine equivalents (mg/d) (Andreasen et al., 2010) (Table 1). Additional details regarding the antipsychotic medication for each patient are provided in Supplementary Table S1. A sample of healthy controls (HC) (n = 23), which was matched to both patient groups by age, gender and education level (Table 1), was also recruited from the faculty in SMHC. All HC did not have a lifetime psychiatric disorder or family history of psychosis in their first-degree relatives. Participants were excluded if they had brain injuries, organic mental disorders, neurologic abnormalities, other serious physical illnesses, dementia, substance abuse or dependence, or contraindications to MRI. The Ethics Committee of SMHC approved the study protocol. Written informed consent was obtained from all subjects prior to study participation.

2.2. Modified electroconvulsive therapy

Bilateral electrical stimulation was administered 3 mornings a week with a Thymatron TMDG instrument (Somatics, Lake Bluff, Ill). Two stimulus electrodes were placed on the left and right temporal scalp. Electroconvulsive therapy conditions were similar for all patients

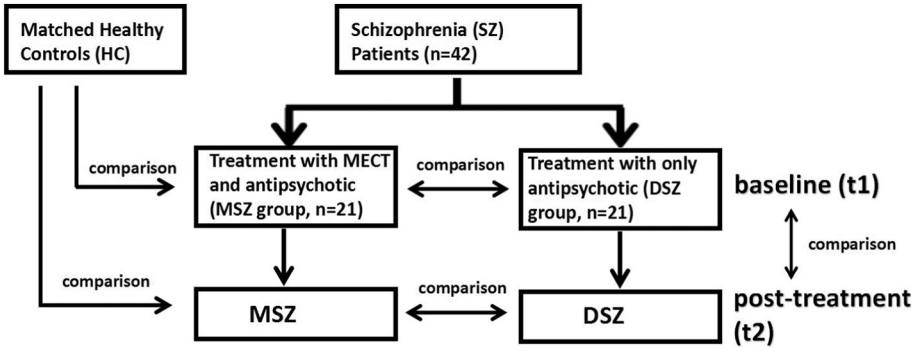

Fig. 1. Study Paradigm. Forty-two patients with acute SZ were divided into two groups according to their treatment strategy. One group (MSZ, n = 21) received 4-weeks of MECT together with antipsychotics; the other (DSZ, n = 21) was treated only with antipsychotics. Twenty-three healthy controls were also included. Structural and functional MRI were scanned twice at baseline and post-treatment.

Table 1
Demographic and clinical data of participants.

Characteristic	MSZ (n = 21) Mean (SD)	DSZ (n = 21) Mean (SD)	P value[a]	HC (n = 23) Mean (SD)
Gender (M/F)[b]	10/11	9/12	0.757	11/12
Age (years)	29.2(7.1)	30.7(7.8)	0.524	31.2 ± 5.9
Education (years)	12.3(3.4)	12.6(2.9)	0.773	13.5 ± 2.5
Handness (left/right)[b]	0/21	0/21	1.000	0/23
Chinese Han nationality[b]	21	21	1.000	23
Married/unmarried/divorced[b]	5/15/1	5/14/2	0.285	13/10/0
Smoking/nonsmoking[b]	3/18	3/18	1.000	7/16
Drinking/nondrinking[b]	0/21	0/21	1.000	3/20
Family history of schizophrenia (yes/no)[b]	8/13	6/15	0.513	0/23
Illness duration (months)[c]	79.8(54.4)	78.7(80.9)	0.435	–
Interval of scans (days)	36.1(10.2)	35.3(14.6)	0.827	–
Chlopromazine equivalents (mg/d)[c]	604.6(565.6)	532.6(461.2)	0.504	–
Baseline PANSS score				
Total	71.6(8.4)	70.8(9.7)	0.673	–
Positive	20.7(2.6)	19.1(3.5)	0.107	–
Negative	19.3(7.4)	17.4(5.1)	0.339	–
General	32.0(3.8)	34.2(5.7)	0.139	–
4-weeks PANSS score				
Total	49.7(9.6)	50.5(12.6)	0.816	–
Positive	10.9(3.0)	12.0(4.7)	0.375	–
Negative	14.6(6.1)	14.0(5.3)	0.768	–
General	24.3(3.33)	24.5(5.4)	0.891	–

[a] P values were obtained using two sample t-tests except where noted.
[b] *P* values were obtained using the chi-square test.
[c] P values were obtained using the Mann-Whitney tests as a result of the substantial variability in each group.

(maximum charge delivered, 504 mC; output current, 0.9 A; frequency, 10–70 Hz; pulse width, 0.5 ms; and maximum stimulus duration, 8 s). Motor convulsions and induced tachycardia were monitored and electroencephalogram and electromyogram were recorded during ECT. Anesthesia was performed with intravenous etomidate (0.21–0.3 mg/kg) and propofol (1.82–2.44 mg/kg). Muscles were relaxed with intravenous succinylcholine (1 mg/kg). Intravenous atropine (0.5 mg) was employed to reduce airway secretion. Patients assigned to the ECT + Drug group did not alter their dosage of antipsychotics during the study period.

The total number of ECT was determined individually by the patient's senior psychiatrist according to both the efficacy and adverse events. In the present study, one session of ECT regularly includes 8–12 ECTs and at least 8 ECTs were administered in all patients irrespective of earlier response. Of 21 patients in ECT + Drug group, 1 received 8 ECTs, 3 received 10 ECTs, 1 received 11 ECTs, and 16 received 12 ECTs. The mean number of ECT was 11.5 ± 1.1.

2.3. Data acquisition and pre-processing

High-resolution T1-weighted images and functional MRI data were acquired using a 3-T Siemens Magnetom Verio Syngo MR B17 scanner. High-resolution T1-weighted images were collected with a magnetization-prepared rapid acquisition gradient echo (MPRAGE) sequence. Functional MRI data were obtained using a gradient echo planar imaging (EPI) sequence. Scanning parameters were provided in the Supplementary information. The patients underwent scanning twice at baseline and after the 4-week treatment, whereas HC were scanned only at baseline.

Functional data pre-processing was performed in SPM 12 (http://www.fil.ion.ucl.ac.uk/spm/) (Ashburner, 2012) and Neuroscience Information Toolbox (http://www.neuro.uestc.edu.cn/NIT.html)(Dong et al., 2018). Conventional pre-processing steps were performed (Huang et al., 2018), which included (1) removal of the first 10 time points; (2) slice-timing correction; (3) realignment; (4) normalization; (5) linear de-trending; (6) nuisance covariates regression; (7) temporally scrubbing; (8) temporal filtering (0.01–0.1 Hz); and (9) smoothing (FWHM = 6 mm). Repeated measure ANOVAs with time as the within-subject factor and group as the between-group factor were used to determine whether there were differences in head-motion (mean FD, max translation and max rotation) from baseline to post-treatment between two groups. Results showed no differences in head-motion. More detailed information can be seen in the Supplementary information.

2.4. Subdivisions of insula using cluster analysis

Previous studies have indicated that the insula may be divided into three subregions, the dAIns, vAIns and PIns (Nelson et al., 2010). According to our previous studies (Chen et al., 2016), we functionally parcellated the left and right insula into three regions separately using the K-means clustering analysis on the fMRI data (Supplementary Information).

2.5. Insular structural analysis

Structural imaging data were firstly processed using standard VBM analysis in SPM 12 (http://www.fil.ion.ucl.ac.uk/spm/). First of all, we check all T1-weighted images for artifacts, and re-oriented the image origins to the anterior commissure. Subsequently, images were segmented into gray matter, WM and CSF, normalized to the MNI space to obtain the GMV maps, and resampled to $2 \times 2 \times 2\,mm^3$. The mean GMV were separately calculated in each region of interest (ROI) of the bilateral dAIns, vAIns and PIns.

2.6. Insular functional connectivity analysis

A voxel-wise FC analysis was conducted with the bilateral dAIns, vAIns and PIns as seed regions. Pearson's correlations between the time course of the seed and that of the whole brain other voxels were calculated and then Fisher's z-transformed to obtain Z scores.

2.7. Statistical analyses

2.7.1. Structural changes

Two sample *t*-tests were performed to compare the differences between the two patient groups at the baseline of t_1. The average GMVs of the entire insula and subregions were analyzed using two-way repeated

measure ANCOVAs with the between-subject factor group (MSZ *vs.* DSZ) and the within-subject factor time (t_1*vs.* t_2). $P < 0.05/6$ was considered significant due to multiple comparisons correction by Bonferroni correction. *Post hoc* analyses of paired *t*-tests were performed to compare the differences between t_1 and t_2 for each patient group. Furthermore, we investigated whether the directions of the GMV changes (t_2-t_1) between the two patient groups were inversed using Wilcoxon signed-rank tests. Moreover, two sample t-tests were applied to compare the differences between the two patient groups at t_2. In addition, we further compared the baseline differences between all the patients and HC by two sample t-tests, and a randomly resampling strategy was performed because of the imbalanced sample size of all patients (42 SZ) and 23 HC. A subsamples of size 23 were randomly generated from all 42 patients at baseline, and each subsample was compared with the HC using two sample t-tests to assess differences of significance. The re-sampling was performed one thousand separately. The percentage was the proportion of these 1000 subsamples with significant differences from the HC. A high percentage represents strong robustness. All tests were performed after controlling for the effects of age, gender, education level and total volume of the whole brain.

2.7.2. Functional connectivity changes

To confirm the distinct FC patterns in the 3 insular subregions, one-sample *t*-tests were performed to determine significant connectivity with the seed. Two sample t-tests were used to compare differences between the two patient groups at baseline. Moreover, a two-way repeated measure ANCOVA was performed. With the aim to determine whether the two treatment methods differentially modulated the insular FC, we focused on the interaction effect between the group and time effects. The main effect of time was also considered to assess the effect of treatment. All analyses based on whole brain FC maps were performed for multiple comparisons correction using a height threshold (min $z > 3.1$, $p < 0.001$) of individual voxel and a cluster size based on Gassian Random Field theory, which corresponds to cluster-level $P_{corrected} = 0.05/6$ due to 6 seeds by Bonferroni correction. Based on these analyses, the peak of each region with a significant interaction effect was selected as a 6 mm radius sphere region of interest (ROI). The mean FC between each ROI and the corresponding insula seed was subsequently extracted for *post hoc* analyses. Two sample t-tests were used to compare the group differences after treatment, and two paired t-tests were employed to compare the differences between t_1 and t_2 for each group. In addition, we further compared the differences between the patient and HC groups *via* a resampling-based strategy mentioned above. All statistical tests were performed controlling for the covariates of age, gender, education level and FD.

2.8. Correlations between insular changes and symptom remission

The mean GMV values of the insular subregions and average FC that exhibited significant interaction effects were extracted. The insular GMV and FC changes were defined as the subtraction (t2 – t1). Following normality tests, Spearman rank correlations were used to assess the relationships between the insular changes and the reductive scores and reductive ratios of the symptoms (PANSS, Positive And Negative Syndrome Scale) for the MSZ. We also investigated the structural and functional co-changes by estimating the correlation between the GMV changes and FC changes in MSZ.

3. Results

3.1. Demographic and clinical data

The two patient groups were not significantly different in terms of age, gender, years of the education, courses of illness, or daily antipsychotic medication dosage during the study. Moreover, the PANSS scores showed no difference between the MSZ and DSZ groups at the baseline (Table 1).

3.2. Insula cluster

Consistent with previous studies (Deen et al., 2011), a cluster analysis segregated the insula into the dAIns, vAIns and PIns. All insular subregions had significant strong FC with the insula and adjacent frontal and temporal cortices (Supplementary Fig. S1).

3.3. Insular structural changes

At baseline, there were no significant differences between the two patient groups *via* two sample *t*-tests (all $p > 0.05$). The repeated ANCOVA indicated the interaction effect of time and group in the bilateral dAIns (right: $F = 11.6$, $p = 0.0017$; left: $F = 7.76$, $p = 0.0086$) and PIns (right: $F = 8.88$, $p = 0.0052$; left: $F = 9.93$, $p = 0.0033$). *Post hoc* analysis indicated that compared with the t_1, the MSZ group had an increased GMV in the bilateral PIns (right: $T = 2.56$, $p = 0.019$; left: $T = 4.32$, $p = 0.00033$). In addition, the bilateral dAIns GMV showed an increasing trend in the MSZ group (right: $T = 1.97$, $p = 0.062$; left: $T = 2.06$, $p = 0.053$). Interestingly, after treatment, the DSZ group exhibited a significantly reduced GMV in the bilateral dAIns, bilateral vAIns and right PIns ($p < 0.05$). The results are presented in Fig. 2 and Table 2. In addition, the two patient groups exhibited inversed alterations following treatment for all insular subregions (Fig. 2 and Table 2). Compared with the HC, the SZ patients at baseline did not show significant differences in the GMV at all insular subregions ($p > 0.05$). After treatment, both the MSZ and DSZ groups had no significant difference in the GMV at all insular subregions compared with the HC ($p > 0.05$). In addition, we also analyzed the GMV changes in the entire insula. Results showed that the two patient groups were not significantly different at baseline. The repeated measure ANCOVAs showed significant interaction effect at the left insula ($F = 8.49$, $p = 0.0062$) and right insula ($F = 12.0$, $p = 0.0014$). *Post hoc* analysis indicated an increased left insula GMV in the MSZ group after treatment ($T = 2.56$, $p = 0.019$). In the DSZ group, the left and right insula exhibited reduced GMV after treatment (left: $T = -2.87$, $p = 0.010$; right: $T = -4.05$, $p = 0.001$). Overall, the structural changes in the entire insula were consistent with the results of insular subregions.

3.4. Insular functional connectivity changes

At baseline, the two patient groups were not significantly different. The repeated measure ANCOVA indicated that the FC between the left PIns and left middle occipital gyrus (MOG) exhibited a significant interaction effect of group and time ($F = 24.4$, $p = 1.4 \times 10^{-5}$). Using *post hoc* paired *t*-test analysis, the MSZ group showed a decreased FC between the left PIns and left MOG at t_2 compared with t_1 ($T = -5.1$, $p = 5.9 \times 10^{-5}$), whereas the DSZ group had no change ($T = 1.4$, $p = 0.18$). In addition, for this functional connection, there was no significant difference between the two patient groups at t_1 ($p > 0.05$) by two sample t-test. However, after different treatments (at t_2), the two patient groups had a significant difference: lower FC in the MSZ group ($T = -3.8$, $p = 0.001$). For another seed of the right PIns, the FC with the left orbitofrontal cortex (OFC) also exhibited a significant interaction effect of group and time ($F = 23.4$, $p = 2.0 \times 10^{-5}$). The *post hoc* paired t-test analysis indicated that compared with the t_1, the patients at t_2 had reduced FC between the right PIns and left OFC for the MSZ group ($T = -5.5$, $p = 2.1 \times 10^{-5}$) with no change for the DSZ group ($T = 1.1$, $p = 0.29$). Interestingly, at t1, the MSZ group had a slightly higher FC than the DSZ group ($T = 2.3$, $p = 0.03$), which did not remain significant after multiple corrections. However, after treatments, the MSZ group showed a severely lower FC than the DSZ group ($T = -4.0$, $p = 0.0007$). These results are presented in Table 3 and Fig. 3.

A significant time effect was also identified in frontal regions,

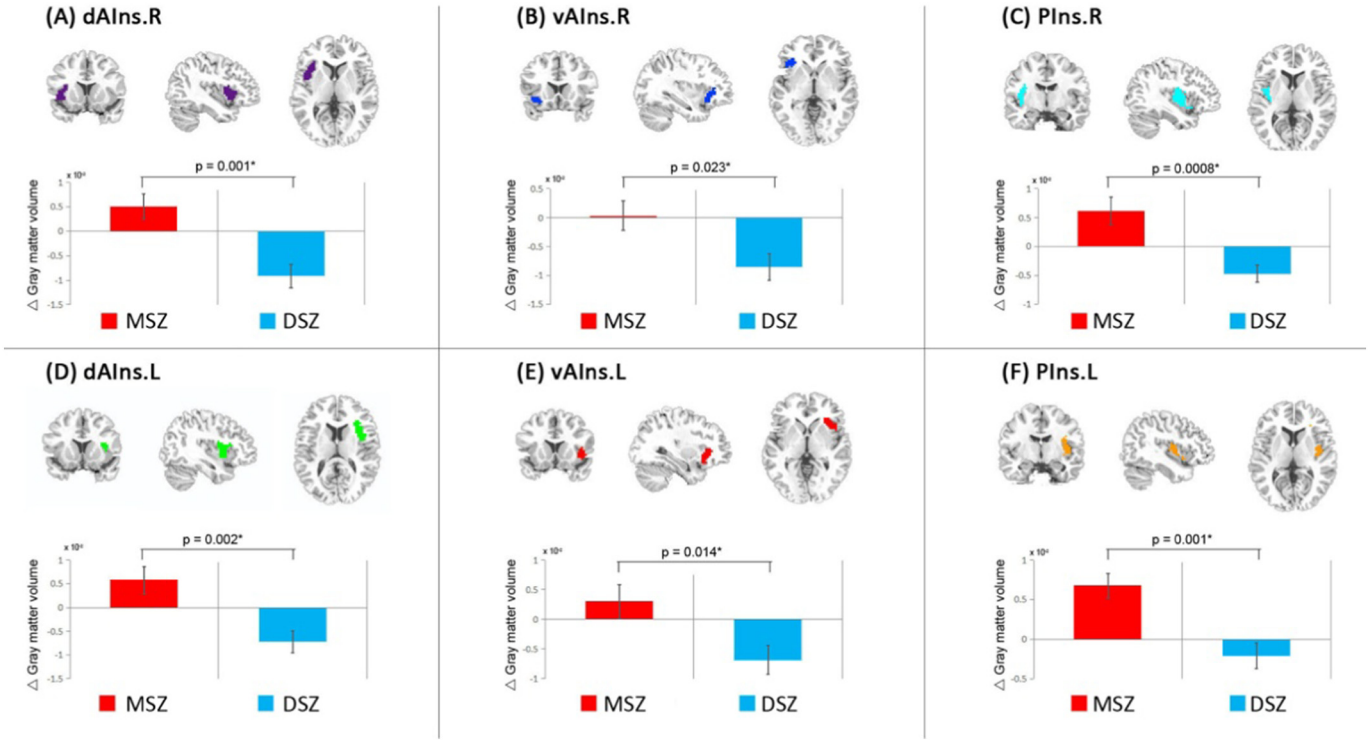

Fig. 2. Gray matter volume changes between pre-treatment (t_1) and post-treatment (t_2) for MSZ group and DSZ group in insular subregions of the (A) right dorsal anterior insula (dAIns.R), (B) right ventral anterior insula (vAIns.R), (C) right posterior insula (PIns.R), (D) left dorsal anterior insula (dAIns.L), (E) left ventral anterior insula (vAIns.L), and (F) left posterior insula (PIns.L). △ indicates the changes following treatment.

Table 2
Gray matter volume changes between t_1 and t_2 in the MSZ and DSZ groups.

Insular subregions	GMV Change (%): Mean (SE)		Paired *t*-test: *p*-value		Wilcoxon signed-rank test: p-value
	MSZ	DSZ	MSZ	DSZ	
dAIns.R	0.51 (0.259)	−0.96 (0.243)	0.062	< **0.001***	**0.001***
vAIns.R	0.04 (0.261)	−0.89 (0.233)	0.893	< **0.001***	**0.023***
PIns.R	0.61 (0.240)	−0.48 (0.157)	**0.019***	**0.006***	< **0.001***
dAIns.L	0.58 (0.282)	−0.80 (0.227)	0.053	**0.002***	**0.002***
vAIns.L	0.30 (0.284)	−0.70 (0.263)	0.298	**0.015***	**0.014***
PIns.L	0.68 (0.157)	−0.26 (0.165)	< **0.001***	0.139	**0.001***

* represents p-value < 0.05.

Table 3
Interaction effect of time and group in whole brain functional connectivity analysis with insular subregions as seeds.

Seed	Region	Coordinates (x, y, z)	Interaction effect		
			F value	P value	Cluster-size
PIns.R	Orbitofrontal cortex	(−42, 33, −6)	23.4	2.0×10^{-5}	76
PIns.L	Middle occipital gyrus	(−42, −78, 27)	24.4	1.4×10^{-5}	61

temporal cortices and cerebellum (Supplementary Table S3 and Fig. S2). The patients at t_2 showed decreased FC between the insular subregions and frontal, temporal and cerebellar regions compared with t_1 (Supplementary Table S4). Detailed information is available in the Supplementary information.

Compared with the HC, the SZ at baseline exhibited increased FC between the bilateral PIns and posterior lobe of cerebellum. After treatment, the MSZ group had enhanced FC between the right PIns and cerebellum, thalamus and postcentral gyrus, as well as increased FC between the left PIns and thalamus and middle occipital gyrus (Supplementary Table S5). The DSZ group showed increased FC between the bilateral PIns and frontal cortex (Supplementary Table S5).

3.5. Correlations between insular changes and symptom remission

In the MSZ group, a significant correlation was observed between the GMV increase in the right PIns and the reductive score of PANSS positive score (rho = 0.667, $p < 0.001$). In addition, correlations were also identified between the GMV increase in the right PIns and the reductive PANSS total score (rho = 0.556, $p = 0.009$), reductive ratio of general psychopathology score (rho = 0.634, $p = 0.002$) and reductive ratio of PANSS total score (rho = 0.578, $p = 0.006$). Moreover, the change of the FC between the right PIns and left OFC was associated with the reductive general psychopathology score (rho = 0.587, $p = 0.005$) and reductive ratios of negative score (rho = 0.560, $p = 0.008$). These correlations remained significant after FDR correlation. Furthermore, the change of the FC between the left PIns and left MOG was correlated with correlation with the reductive negative score (rho = 0.460, $p = 0.036$). We did not identify correlations between the GMV increase in the left PIns and disease severity changes. These results are shown in Fig. 4. In addition, a structural and functional co-change was observed in the left PIns. Increased GMV in the left PIns had a negative correlation with reduced FC between left PIns and right MTG ($R = -0.468$, $p = 0.0326$).

4. Discussion

This investigation found insular structural and FC changes in SZ

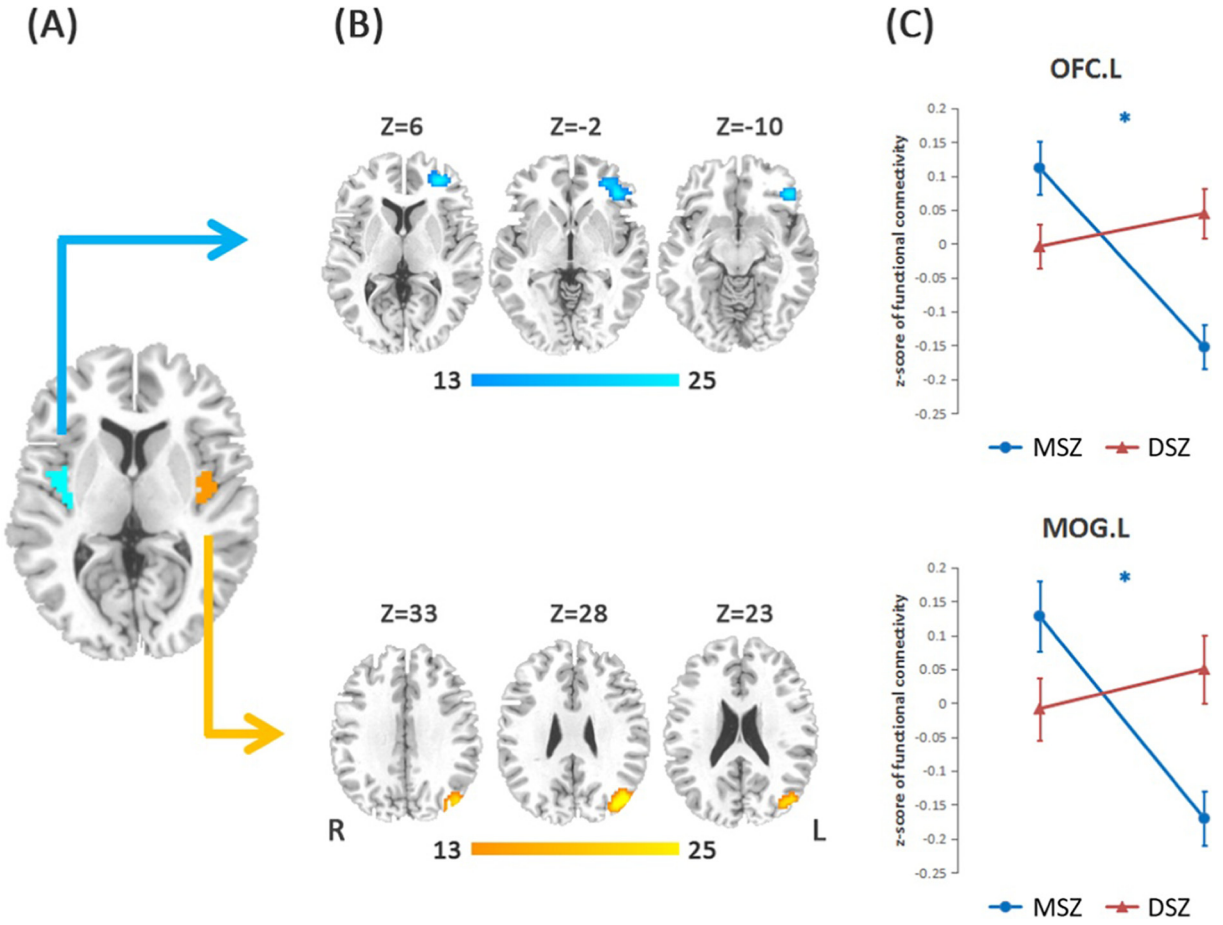

Fig. 3. Insular functional connectivity analysis. (A) Seeds of right and left PIns. (B) Interaction effect of time and group. (C) Results of *post hoc* analysis. OFC: orbitofrontal cortex; MOG: middle occipital gyrus.

following MECT. First, compared with the patients with drug treatment only, MSZ group showed a distinctly increased GMV in bilateral PIns. Furthermore, the increase associated with the symptom improvement. Second, the MSZ group, but not the DSZ group, exhibited decreased FC between the PIns and OFC as well as MOG after treatment; moreover, these changes were significantly related to symptom remission.

Over the previous decade, structural MRI has consistently shown the decreased insular gray matter in different types of patients with SZ (Ellison-Wright et al., 2008; Honea et al., 2005), such as first-episode and chronic SZ (Chan et al., 2011). Thus, restraining from the insular cortex deficit would be a crucial target of an effective treatment approach in SZ. In the current study, we did not observe significant GMV differences between SZ and HC at insular subregions. We speculated that the heterogeneity such as the course of illness, clinical symptoms and antipsychotics medication in the SZ sample may be the reason why no changes between SZ and HC. A previous study has illustrated an increased insular GMV following MECT in patients with late life depression (Bouckaert et al., 2016), which suggests that the insula would be included in the MECT effect. Consistent with our hypothesis, the current study indicated that the MECT induced an increase in insular volume. It is noteworthy that this study also illustrated a significant correlation between the right PIns GMV increase and positive symptom improvement. Interestingly, a previous study indicated that more decreased insular GMV was linked to worse positive symptoms in SZ (Pressler et al., 2005). In addition, SZ patients with only antipsychotic medication showed a reduced GMV in most insular subregions in this study. The decreased insular volume has been identified in the SZ patients with antipsychotics; this study indicated that a short-time course of therapy with drugs could also induce a reduction in insular volume. Taken together, the specific increase in the insular volume may be one of the MECT action mechanisms.

In addition, this study identified specific MECT-induced changes: the decreased FC of the PIns with the OFC and MOG following treatment. These alterations in response to MECT in SZ are understandable considering the neuroimaging evidence for an involvement of the orbitofrontal cortices and primary cortex in the neural changes associated with MECT (van Waarde et al., 2015; Xia et al., 2018). Moreover, the orbitofrontal and primary cortex dysfunctions are well-established in SZ, supported by functional and structural findings (Chen et al., 2017; Jiang et al., 2018b; Kaufmann et al., 2015), and the two regions mediate key symptoms including positive and negative, as well as cognitive dysfunction of SZ (Chen et al., 2015). The PIns, as a core brain region for processing multimodal sensory information, is supposed to anatomically and functionally connect with the somatosensory and motor cortices (Uddin, 2015). The decreased FC of the PIns with the sensor area and prefrontal cortex identified in the current study may suggest the modulation effect of MECT on the integration of interoceptive events and external stimuli. In addition, a relationship between the FC changes and symptom reductive scores was observed, which further indicated that FC contributed to the understanding of pathophysiology in SZ.

Furthermore, we identified a significantly correlation between structural and functional changes in the left PIns. The cellular foundation that underlies these changes may include neurogenesis, synaptogenesis and gliogenesis, changes in glial number and morphology, and angiogenesis (Zatorre et al., 2012). Thus, this interesting finding may suggest compensatory processes of volume and connectivity changes, that is, neurogenesis and gliogenesis may be analogous to the

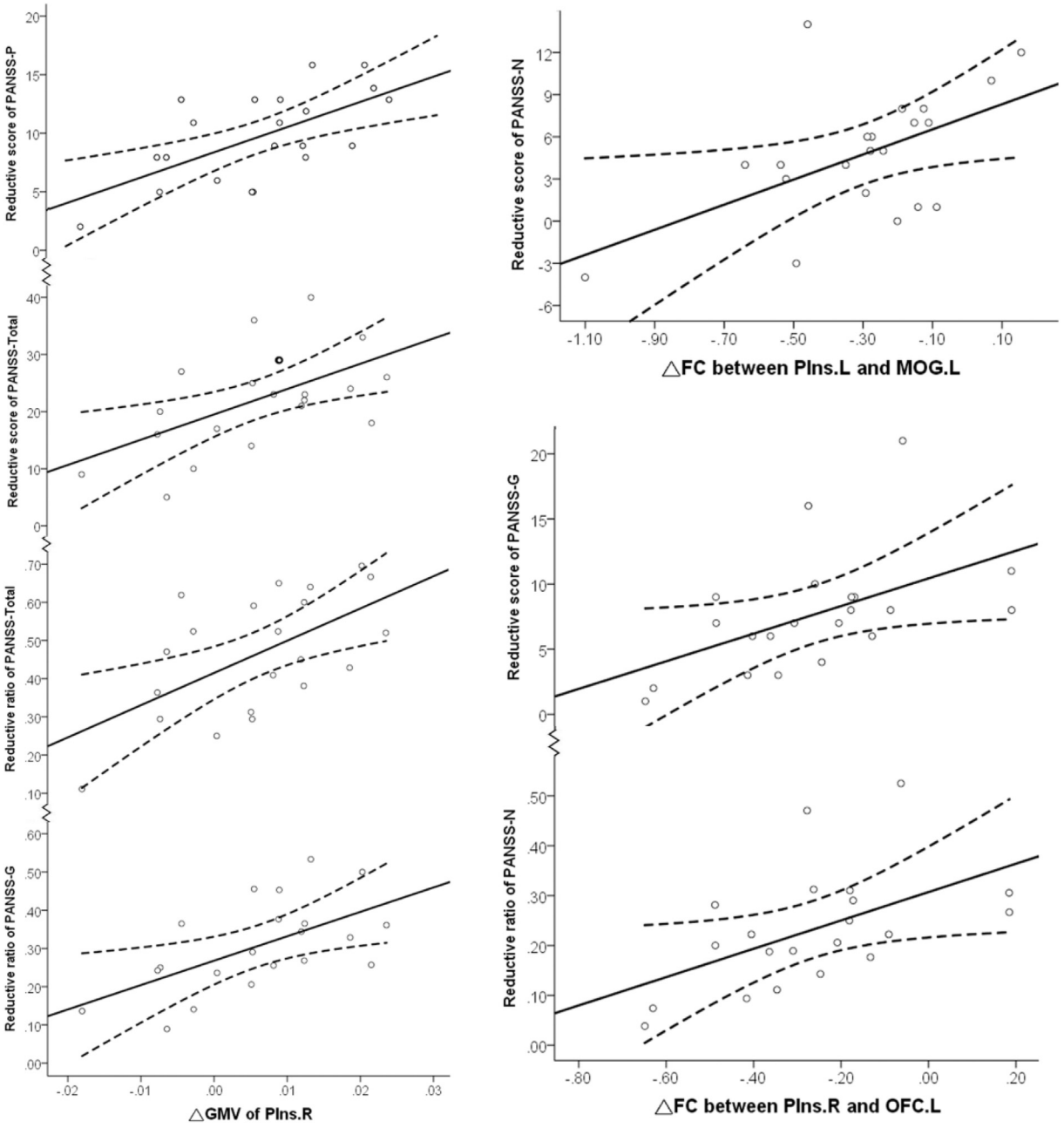

Fig. 4. Correlations between gray matter volume/functional connectivity changes in the PIns and disease severity reduction for the MSZ group.

volume and synaptogenesis may correspond to the FC.

This study must be interpreted with caution because of several limitations. First, the participants included medicated and chronic patients. SZ is a progressive mental disorder, and the long duration of the illness may have a neurotoxic effect on the gray matter (Perkins et al., 2005). Moreover, antipsychotic drugs have been demonstrated to significantly confound the findings of both anatomical and functional neuroimaging studies (He et al., 2018a, 2018b; Lui et al., 2010; Yang et al., 2018). Second, the allocation of schizophrenia patients to ECT or drug group was not randomized, which possibly brought a bias in favoring ECT. Although the matched comparison patients enabled us to control for the effect induced by the antipsychotic medication, the effects of concomitant drug medications during the MECT course could not be completely ruled out. Third, the neuropsychological assessments were not evaluated; thus, we could not assess the associations between the changes in cognitive and brain changes. With a focus on cognitive changes following MECT (Semkovska and McLoughlin, 2010), detailed assessments should be employed in the future, such as the Digit Span test and Stroop test (attention and executive functioning), as well as the Digit Symbol test (processing speed). Fourth, in consideration of the high relapse rates after MECT (Pompili et al., 2013), it is likely that the changes following MECT may return to the “baseline”. Therefore, longitudinal studies with > 2 MRI scanning time points are required to determine whether the MECT-induced change is a transient phenomenon. Finally, we cannot excluded the effect of edema in the interpretation of the findings on VBM because we did not assess T2 relaxation time (corresponding to water content) after MECT.

5. Conclusion

In conclusion, this study provided evidence for both structural and functional changes in the insula induced by MECT in SZ. A distinctly increased GMV in bilateral PIns and decreased FC between the PIns and OFC as well as MOG were observed in SZ following MECT.

Furthermore, these insular changes associated with the symptom improvements.

Conflict of interest

There is no conflict of interest.

Contributors

JJW, CL designed the experiment and wrote the protocol. YCJ, HH, XKL, DBD and SSJ managed the literature searches and undertook the statistical analysis; MQX and JJW collected the image data and clinical information; YCJ, CL and MQX wrote the first draft of the manuscript; YYT, CBL, JJW, CL and DZY reviewed this article critically and gave final approval of the version of the article to be published. All authors contributed to and have approved the final manuscript.

Ethical statement

The study was approved by the Ethics Committee of Shanghai Mental Health Center, Shanghai, China. Written informed consent was obtained after a complete description of the study for each participant.

Acknowledgements

This study was funded by grants from the National Nature Science Foundation of China (81471638, 81671332, 81571759, 81861128001), the '111' Project (B12027), grants from Ministry of Science and Technology of China (2016YFC1306800), Project of Scientific Expenses of the Ministry of Education (2017PT14), SHSMU-ION Research Center for Brain Disorders (2015NKX001), and the Project of Science and Technology Department of Sichuan Province (2017HH0001, 2017SZ0004).

Appendix A. Supplementary data

Supplementary data to this article can be found online at https://doi.org/10.1016/j.pnpbp.2018.09.009.

References

Abbott, C.C., Jones, T., Lemke, N.T., Gallegos, P., McClintock, S.M., Mayer, A.R., Bustillo, J., Calhoun, V.D., 2014. Hippocampal structural and functional changes associated with electroconvulsive therapy response. Transl. Psychiatry 4, e483.

Abraham, K.R., Kulhara, P., 1987. The Efficacy of Electroconvulsive Therapy in the Treatment of Schizophrenia. A Comparative Study. The British Journal of Psychiatry : The Journal of Mental Science 151. pp. 152–155.

Andrade, C., Bolwig, T.G., 2014. Electroconvulsive therapy, hypertensive surge, blood-brain barrier breach, and amnesia: exploring the evidence for a connection. J. ECT 30 (2), 160–164.

Andreasen, N.C., Pressler, M., Nopoulos, P., Miller, D., Ho, B.C., 2010. Antipsychotic dose equivalents and dose-years: a standardized method for comparing exposure to different drugs. Biol. Psychiatry 67 (3), 255–262.

Ashburner, J., 2012. SPM: a history. NeuroImage 62 (2), 791–800.

Bouckaert, F., Sienaert, P., Obbels, J., Dols, A., Vandenbulcke, M., Stek, M., Bolwig, T., 2014. ECT: its brain enabling effects a review of electroconvulsive therapy-induced structural brain plasticity. J. ECT 30 (2), 143–151.

Bouckaert, F., De Winter, F.L., Emsell, L., Dols, A., Rhebergen, D., Wampers, M., Sunaert, S., Stek, M., Sienaert, P., Vandenbulcke, M., 2016. Grey matter volume increase following electroconvulsive therapy in patients with late life depression: a longitudinal MRI study. J. Psychiatry Neurosci. 41 (2), 105–114.

Cao, W., Luo, C., Zhu, B., Zhang, D., Dong, L., Gong, J., Gong, D., He, H., Tu, S., Yin, W., Li, J., Chen, H., Yao, D., 2014. Resting-state functional connectivity in anterior cingulate cortex in normal aging. Front. Aging Neurosci. 6, 280.

Chan, R.C., Di, X., McAlonan, G.M., Gong, Q.Y., 2011. Brain anatomical abnormalities in high-risk individuals, first-episode, and chronic schizophrenia: an activation likelihood estimation meta-analysis of illness progression. Schizophr. Bull. 37 (1), 177–188.

Chang, L.J., Yarkoni, T., Khaw, M.W., Sanfey, A.G., 2013. Decoding the role of the insula in human cognition: functional parcellation and large-scale reverse inference. Cereb. Cortex 23 (3), 739–749.

Chen, X., Duan, M., Xie, Q., Lai, Y., Dong, L., Cao, W., Yao, D., Luo, C., 2015. Functional disconnection between the visual cortex and the sensorimotor cortex suggests a potential mechanism for self-disorder in schizophrenia. Schizophr. Res. 166 (1–3), 151–157.

Chen, X., Duan, M., He, H., Yang, M., Klugah-Brown, B., Xu, H., Lai, Y., Luo, C., Yao, D., 2016. Functional abnormalities of the right posterior insula are related to the altered self-experience in schizophrenia. Psychiatry Res. 256, 26–32.

Chen, X., Liu, C., He, H., Chang, X., Jiang, Y., Li, Y., Duan, M., Li, J., Luo, C., Yao, D., 2017. Transdiagnostic differences in the resting-state functional connectivity of the prefrontal cortex in depression and schizophrenia. J. Affect. Disord. 217, 118–124.

Deen, B., Pitskel, N.B., Pelphrey, K.A., 2011. Three systems of insular functional connectivity identified with cluster analysis. Cereb. Cortex 21 (7), 1498–1506.

Dong, D., Wang, Y., Chang, X., Luo, C., Yao, D., 2017. Dysfunction of Large-Scale Brain Networks in Schizophrenia: a Meta-analysis of Resting-State Functional Connectivity. Schizophr. Bull. 44 (1), 168–181.

Dong, L., Luo, C., Liu, X., Jiang, S., Li, F., Feng, H., Li, J., Gong, D., Yao, D., 2018. Neuroscience Information Toolbox: an Open Source Toolbox for EEG–fMRI Multimodal Fusion Analysis. Front. Neuroinformatics 12, 56.

Ellison-Wright, I., Glahn, D.C., Laird, A.R., Thelen, S.M., Bullmore, E., 2008. The anatomy of first-episode and chronic schizophrenia: an anatomical likelihood estimation meta-analysis. Am. J. Psychiatry 165 (8), 1015–1023.

Fochtmann, L.J., 2016. Evidence for the continuing Benefits of Electroconvulsive Therapy. Am. J. Psychiatry 173 (11), 1071–1072.

He, H., Luo, C., Luo, Y., Duan, M., Yi, Q., Biswal, B.B., Yao, D., 2018a. Reduction in gray matter of cerebellum in schizophrenia and its influence on static and dynamic connectivity. Human brain Mapping Online. 1–12. https://doi.org/10.1002/hbm.24391.

He, H., Yang, M., Duan, M.J., Chen, X., Lai, Y.X., Xia, Y., Shao, J.M., Biswal, B.B., Luo, C., Yao, D.Z., 2018b. Music intervention leads to increased Insular Connectivity and improved Clinical Symptoms in Schizophrenia. Front. Neurosci. Switz 11.

Honea, R., Crow, T.J., Passingham, D., MacKay, C.E., 2005. Regional deficits in brain volume in schizophrenia: a meta-analysis of voxel-based morphometry studies. Am. J. Psychiatry 162 (12), 2233–2245.

Huang, H., Jiang, Y., Xia, M., Tang, Y., Zhang, T., Cui, H., Wang, J., Li, Y., Xu, L., Curtin, A., Sheng, J., Jia, Y., Yao, D., Li, C., Luo, C., Wang, J., 2018. Increased resting-state global functional connectivity density of default mode network in schizophrenia subjects treated with electroconvulsive therapy. Schizophr. Res. 197, 192–199.

Jiang, Y., Duan, M., Chen, X., Chang, X., He, H., Li, Y., Luo, C., Yao, D., 2017. Common and distinct dysfunctional patterns contribute to triple network model in schizophrenia and depression: a preliminary study. Prog. Neuropsychopharmacol. Biol. Psychiatry 79 (Pt B), 302–310.

Jiang, Y., Luo, C., Li, X., Duan, M., He, H., Chen, X., Yang, H., Gong, J., Chang, X., Woelfer, M., Biswal, B.B., Yao, D., 2018a. Progressive Reduction in Gray Matter in patients with Schizophrenia Assessed with MR Imaging by using Causal Network Analysis. Radiology 171832.

Jiang, Y., Luo, C., Li, X., Li, Y., Yang, H., Li, J., Chang, X., Li, H., Yang, H., Wang, J., Duan, M., Yao, D., 2018b. White-matter functional networks changes in patients with schizophrenia. NeuroImage. https://doi.org/10.1016/j.neuroimage.2018.04.018.

Kaufmann, T., Skatun, K.C., Alnaes, D., Doan, N.T., Duff, E.P., Tonnesen, S., Roussos, E., Ueland, T., Aminoff, S.R., Lagerberg, T.V., Agartz, I., Melle, I.S., Smith, S.M., Andreassen, O.A., Westlye, L.T., 2015. Disintegration of Sensorimotor Brain Networks in Schizophrenia. Schizophr. Bull. 41 (6), 1326–1335.

Lui, S., Li, T., Deng, W., Jiang, L., Wu, Q., Tang, H., Yue, Q., Huang, X., Chan, R.C., Collier, D.A., Meda, S.A., Pearlson, G., Mechelli, A., Sweeney, J.A., Gong, Q., 2010. Short-term effects of antipsychotic treatment on cerebral function in drug-naive first-episode schizophrenia revealed by "resting state" functional magnetic resonance imaging. Arch. Gen. Psychiatry 67 (8), 783–792.

Luo, C., Tu, S., Peng, Y., Gao, S., Li, J., Dong, L., Li, G., Lai, Y., Li, H., Yao, D., 2014. Long-term effects of musical training and functional plasticity in salience system. Neural Plasticity 2014, 180138.

Menon, V., 2011. Large-scale brain networks and psychopathology: a unifying triple network model. Trends Cogn. Sci. 15 (10), 483–506.

Moran, L.V., Tagamets, M.A., Sampath, H., O'Donnell, A., Stein, E.A., Kochunov, P., Hong, L.E., 2013. Disruption of anterior insula modulation of large-scale brain networks in schizophrenia. Biol. Psychiatry 74 (6), 467–474.

Nelson, S.M., Dosenbach, N.U., Cohen, A.L., Wheeler, M.E., Schlaggar, B.L., Petersen, S.E., 2010. Role of the anterior insula in task-level control and focal attention. Brain Struct. Funct. 214 (5–6), 669–680.

Palaniyappan, L., Simmonite, M., White, T.P., Liddle, E.B., Liddle, P.F., 2013. Neural primacy of the salience processing system in schizophrenia. Neuron 79 (4), 814–828.

Perkins, D.O., Gu, H., Boteva, K., Lieberman, J.A., 2005. Relationship between duration of untreated psychosis and outcome in first-episode schizophrenia: a critical review and meta-analysis. Am. J. Psychiatry 162 (10), 1785–1804.

Petrides, G., Malur, C., Braga, R.J., Bailine, S.H., Schooler, N.R., Malhotra, A.K., Kane, J.M., Sanghani, S., Goldberg, T.E., John, M., Mendelowitz, A., 2015. Electroconvulsive therapy augmentation in clozapine-resistant schizophrenia: a prospective, randomized study. Am. J. Psychiatry 172 (1), 52–58.

Pompili, M., Lester, D., Dominici, G., Longo, L., Marconi, G., Forte, A., Serafini, G., Amore, M., Girardi, P., 2013. Indications for electroconvulsive treatment in schizophrenia: a systematic review. Schizophr. Res. 146 (1–3), 1–9.

Pressler, M., Nopoulos, P., Ho, B.C., Andreasen, N.C., 2005. Insular cortex abnormalities in schizophrenia: Relationship to symptoms and typical neuroleptic exposure. Biol. Psychiatry 57 (4), 394–398.

Redlich, R., Opel, N., Grotegerd, D., Dohm, K., Zaremba, D., Burger, C., Munker, S., Muhlmann, L., Wahl, P., Heindel, W., Arolt, V., Alferink, J., Zwanzger, P., Zavorotnyy, M., Kugel, H., Dannlowski, U., 2016. Prediction of Individual Response to Electroconvulsive Therapy via Machine Learning on Structural magnetic Resonance Imaging Data. JAMA Psychiatr. 73 (6), 557–564.

Semkovska, M., McLoughlin, D.M., 2010. Objective cognitive performance associated

with electroconvulsive therapy for depression: a systematic review and meta-analysis. Biol. Psychiatry 68 (6), 568–577.
Takamiya, A., Chung, J.K., Liang, K.C., Graff-Guerrero, A., Mimura, M., Kishimoto, T., 2018. Effect of electroconvulsive therapy on hippocampal and amygdala volumes: systematic review and meta-analysis. Br. J. Psychiatry 212 (1), 19–26.
Thomann, P.A., Wolf, R.C., Nolte, H.M., Hirjak, D., Hofer, S., Seidl, U., Depping, M.S., Stieltjes, B., Maier-Hein, K., Sambataro, F., Wustenberg, T., 2017. Neuromodulation in response to electroconvulsive therapy in schizophrenia and major depression. Brain Stimul. 10 (3), 637–644.
Uddin, L.Q., 2015. Salience processing and insular cortical function and dysfunction. Nat. Rev. Neurosci. 16 (1), 55–61.
van Waarde, J.A., Scholte, H.S., van Oudheusden, L.J., Verwey, B., Denys, D., van Wingen, G.A., 2015. A functional MRI marker may predict the outcome of electroconvulsive therapy in severe and treatment-resistant depression. Mol. Psychiatry 20 (5), 609–614.
Wylie, K.P., Tregellas, J.R., 2010. The role of the insula in schizophrenia. Schizophr. Res. 123 (2–3), 93–104.
Xia, M., Wang, J., Sheng, J., Tang, Y., Li, C., Lim, K., He, B., Li, C., Xu, Y., Wang, J., 2018. Effect of Electroconvulsive Therapy on Medial Prefrontal γ-Aminobutyric Acid among Schizophrenia patients: a Proton magnetic Resonance Spectroscopy Study. J. ECT. https://doi.org/10.1097/yct.0000000000000507.
Yang, M., He, H., Duan, M., Chen, X., Chang, X., Lai, Y., Li, J., Liu, T., Luo, C., Yao, D., 2018. The Effects of Music intervention on Functional Connectivity Strength of the Brain in Schizophrenia. Neural Plasticity 2018.
Zatorre, R.J., Fields, R.D., Johansen-Berg, H., 2012. Plasticity in gray and white: neuroimaging changes in brain structure during learning. Nat. Neurosci. 15 (4), 528–536.